Microstructure of Maleic Anhydride Grafted Polyethylene by High-Resolution Solution-State NMR and FTIR Spectroscopy

Liqun Yang, Farao Zhang, Takashi Endo, and Takahiro Hirotsu*

Institute for Marine Resources and Environment Research, National Institute of Advanced Industrial Science and Technology (AIST), 2217-14 Hayashi-cho, Takamatsu 761-0395, Japan

Received April 2, 2002; Revised Manuscript Received May 6, 2003

ABSTRACT: The microstructure of maleic anhydride (MA) grafted polyethylene (PE), MA-*g*-PE, has been successfully characterized by high-resolution NMR and FT-IR spectroscopy. The carbonyl asymmetric and symmetric stretchings of MA-*g*-PE exhibit lower shifts with an increase in the grafting degree of MA, suggesting stronger inductive interactions between different grafts in a solid state. The ^{1}H and ^{13}C NMR spectroscopy of [2,3-$^{13}C_2$]MA grafted PE with a low molecular weight (lmPE), [2,3-$^{13}C_2$]MA-*g*-lmPE, demonstrates that [2,3-$^{13}C_2$]MA-*g*-lmPE contains fewer succinic anhydride (SA) oligomeric grafts with a terminal unsaturated MA ring (oligo-MA) in addition to more SA oligomeric grafts terminated with a saturated SA ring (oligo-SA), the only structure that had been observed prior to this study. The formation of oligo-MA and oligo-SA can be explained by a mechanism based on two different termination processes: disproportionation between a grafting radical and a macroradical on a secondary carbon in lmPE or another grafting radical as well as hydrogen abstraction of a grafting radical from a secondary carbon on lmPE.

Introduction

Polyethylene (PE) has been extensively used in plastics because of its low-cost versatility. But large quantities of waste PE products have been causing the serious environmental problem that it takes a long time to make PE decompose. Recently, growing interest has been directed to the development of novel composites of PE with natural polymers,[1−5] which are promising as new environmental protection plastics. Maleic anhydride (MA) grafted PE, MA-*g*-PE, is very important in the enhancement of compatibility between nonpolar PE and natural polar materials like cellulose and chitin. Accordingly, clarification of the molecular structure of MA-*g*-PE has been required for the design of novel composites.[6]

The modifications of PE with MA through a free-radical reaction in both solution and melt processes have been widely investigated.[7−11] It has been generally accepted that primary free radicals generated by initiators first abstract hydrogen atoms from the PE backbone to form macroradicals, after which the macroradicals undergo grafting with MA or cross-linking between themselves.[12] From the theory of grafting of MA on PE proposed by Gaylord and Mehta,[11] the macroradicals with different average graft chain lengths ($m + 1$ and $n + 1$) probably undergo three main terminations: disproportionation, hydrogen abstraction, and coupling (Scheme 1). MA being a strong electron acceptor causes a tendency toward disproportionation and hydrogen abstraction rather than coupling,[13,14] suggesting that the possibility of structure **III** is very small. However, the lack of well-confirmed experimental evidence has left obscure the molecular structure of MA groups grafted onto PE, mainly owing to the low graft degree.[12]

Roover and Sclavons et al.[15,16] have investigated MA grafted polypropylene (MA-*g*-PP) with FTIR by using a series of model compounds, such as *n*-octadecylsuccinic anhydride and poly(MA). They reported that single succinic anhydride (SA) and oligomeric SA grafts exist in MA-*g*-PP and calculated the average length of oligomeric SA grafts. But there has been little progress in the further characterization of the microstructure of MA grafts onto PE from FTIR.

Recently, Heinen et al. [13] synthesized [2,3-$^{13}C_2$]MA-*g*-PE both in solution and in melt systems, including high-density PE (HDPE) and low-density PE (LDPE). From noise-decoupled and 1D inadequate ^{13}C NMR spectroscopy, they found that MA groups grafted onto HDPE and LDPE are in the form of single SA and short oligomeric SA, the average chain length of which is about 1−2 when the grafting is carried out with an MA amount of 10 wt % PE.

This study describes the molecular structure of MA grafted PE, MA-*g*-PE, which was synthesized in solution, as measured with solution-state NMR and FTIR spectroscopy. We have demonstrated for the first time the formation of the fewer SA oligomeric grafts with a terminal unsaturated MA ring (oligo-MA; structure **I** in Scheme 1) in addition to the more SA oligomeric grafts terminating in a saturated SA ring (oligo-SA; structure **II** in Scheme 1),[12] the only structure that had been observed prior to this study, on [2,3-$^{13}C_2$]MA grafted low molecular weight PE (lmPE), [2,3-$^{13}C_2$]MA-*g*-lmPE. A grafting mechanism with two different termination processes is described to explain the formation of oligo-MA and oligo-SA.

Experimental Section

Reagents. [2,3-$^{13}C_2$]MA, isotopically enriched with 99% ^{13}C, and 1,1,2,2-tetrachloroethane-d_2 were purchased from ISOTEC Inc. Di-*tert*-butyl peroxide (DTBP), benzoyl peroxide (BPO), and four kinds of PE were from Aldrich: high-density PE (HDPE1; M_W: ca. 125 000; melt index: 0.25), high-density PE (HDPE2; melt index: 36), low-density PE (LDPE; melt index: 55), and low molecular weight PE (lmPE; M_W: ca. 4000; M_n: ca. 1700). *o*-Dichlorobenzene (*o*-DCB), dehydrated acetone (water content < 50 ppm), tetrahydrofuran (THF), and hexamethyldisiloxane (HMDS) were bought from Wako. Standard polystyrene was obtained commercially from Showa Denko K.K. *n*-Octadecylsuccinic anhydride was purchased from Tokyo Kasei Organic Chemicals Inc.

* Corresponding author. E-mail: takahiro-hirotsu@aist.go.jp.

10.1021/ma020527r CCC: $25.00
Published on Web 06/07/2003

Scheme 1. Termination of MA-*g*-PE Macroradicals

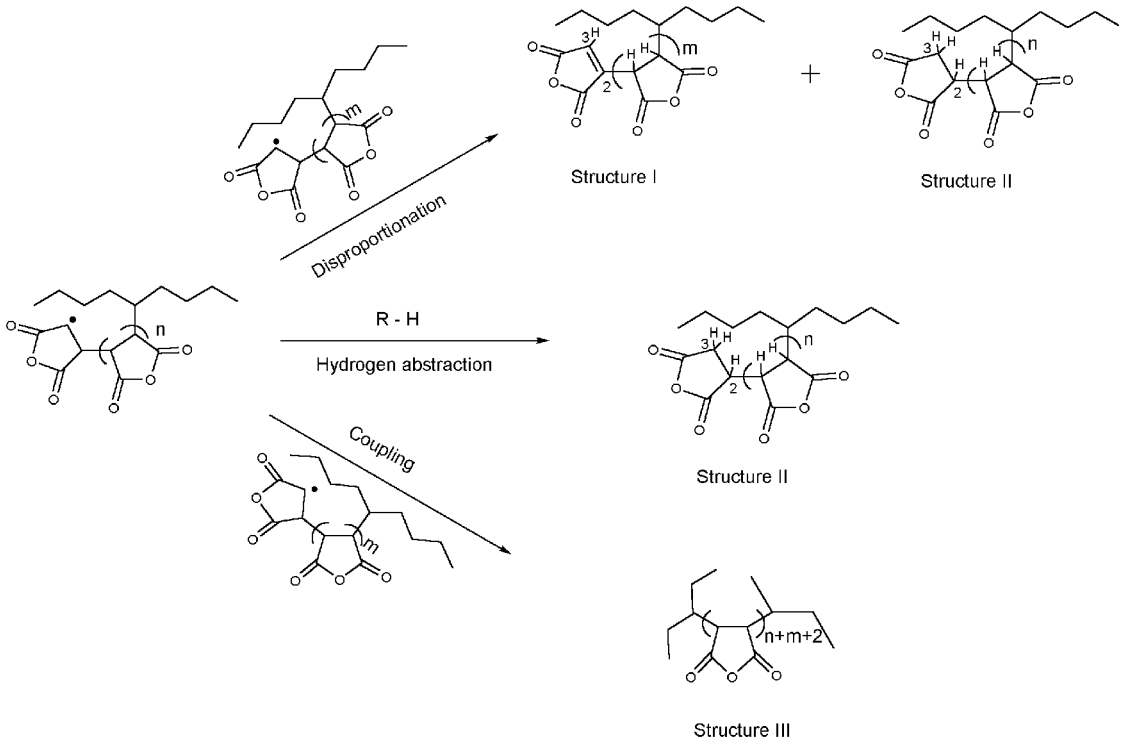

Synthesis of MA-*g*-PE. The graft copolymerization was carried out in a three-neck round-bottom flask equipped with a condenser, a thermometer, and a nitrogen gas inlet, while stirring with a magnetic bar. The temperature was maintained in an oil bath with a contact thermometer. One gram of PE was completely dissolved in *o*-DCB (20 mL) at 140 °C, and the polymer solution was maintained at a temperature of 150−190 °C. After a solution of MA (0.0025−0.35 g) in *o*-DCB (5 mL) followed by a solution of DTBP (0.01−0.1 g) in *o*-DCB (5 mL) was added to the PE solution, the reaction was carried out for a given time of 0.5−2 h. Addition of acetone (100 mL) to the reaction mixture resulted in the precipitation of a crude product. The crude product was purified by dissolving in *o*-DCB, precipitating with 5−10 times volume of boiling acetone with stirring, and filtrating, until no MA, homopolymer of MA, and initiator was observed in the filtrate by gel permeation chromatography (GPC). The pure product was dried in a vacuum at 100 °C overnight.

Synthesis of Poly(MA).[17] A mixture of MA (5 g) and BPO (0.25 g) in 10 mL of benzene was put in a one-neck round-bottom flask. After a procedure involving cooling with liquid nitrogen, evacuating, and warming to room temperature was repeated three times, the flask was sealed under vacuum. The homopolymerization was carried out at 80 °C for 32 h. The crude product was purified by dissolving in acetone and precipitating with benzene two times, and the pure product was dried in a vacuum at 60 °C overnight (M_w = 1486, M_n = 1195, M_w/M_n = 1.243 by GPC).

GPC Analysis. The molecular weight of poly(MA) and the purity of MA-*g*-PE were determined with a GPC system constituted of a Waters 600E pump, a Shimadzu refractive index detector RID-10A, and two columns of PLgel 3 μm 100 A (Polymer Laboratories Ltd.). The mobile phase was THF at 25 °C. The sample concentration was 6 mg/mL, the injection volume was 50 μl, and the flow speed was 0.5 mL/min.

FTIR Measurement. FTIR spectra were recorded on a Perkin-Elmer spectrum 2000 FTIR spectrometer from 4000 to 400 cm^{-1} at a 0.5 cm^{-1} resolution for 100 scans. The samples were prepared by compression-molding 0.1−0.2 g of MA-*g*-PE between Teflon-film coated steel sheets to form films of 20−100 μm, using a Takujou laboratory press (Toyoseiki Co.) under a 180 kgf/cm^2 force at 110−190 °C for 30 s.

NMR Measurements. Solution NMR spectra were obtained on a Varian Inova 400 spectrometer at 85 °C. A sample (175 mg) was dissolved in 0.7 mL of 1,1,2,2-tetrachloroethane-d_2 in a 5 mm diameter NMR tube. ^{1}H spectra were performed at 399.80 Hz and ^{13}C NMR spectra at 100.53 Hz. ^{13}C NMR chemical shifts were referred internally to that of the major backbone methylene carbon, which was 30.00 ppm from TMS,[18] and ^{1}H chemical shifts referred to internal standard HMDS at 0.06 ppm.

Quantitative Inverse-Gated ^{1}H Decoupled ^{13}C NMR. The fast inversion recovery technique[19] was employed to measure the spin−lattice relaxation time (T_1). A relaxation-delay time of 10 s (>5 T_1 of the labeled carbons) was used to obtain the complete relaxation and a gated coupling technique to produce spectra without the nuclear Overhauser effect (NOE).

DEPT. DEPT spectra were recorded with J_{H-C} of 140 Hz, a relaxation-relay time of 2 s, proton magnetic vector rotation angles θ = 45° giving approximately equal excitation of all protonated carbons, θ = 90° exciting CH's only or mainly, and θ = 135° giving CH's and CH_3's up, and CH_2's down.

H, C-COSY. An acquisition time of 0.084 s, a delay of 1.00 s, 400 transients per increment, 256 increments, and J_{H-C} of 140 Hz were used.

COSY. The COSY experiment was carried out using a delay of 0.185 s, 252 transients per increment, and 256 increments.

Results and Discussion

IR spectra of MA-*g*-PE are shown in Figure 1. MA-*g*-PE exhibits absorptions at 1864−1860 cm^{-1} {the asymmetric stretching of carbonyl ν_{as}(C=O)}, 1786−1784 cm^{-1} {the symmetric stretching of carbonyl ν_s(C=O)}, 1224 cm^{-1} {the asymmetric ring stretching ν(=C−O−C=)}, and 1064 cm^{-1} (curves a−c) and 1051 cm^{-1} (curve d) {the symmetric ring stretching ν(=C−O−C=)}, characteristic of cyclic ethers.[20,21] The appearance of the ring stretching vibration of saturated cyclic five-membered anhydride at around 919 cm^{-1} instead of two sharp bands at 867 and 892 cm^{-1} due to the C=C stretching of monomeric MA[22] further confirms that MA monomers are grafted onto PE.[23] A strong absorption

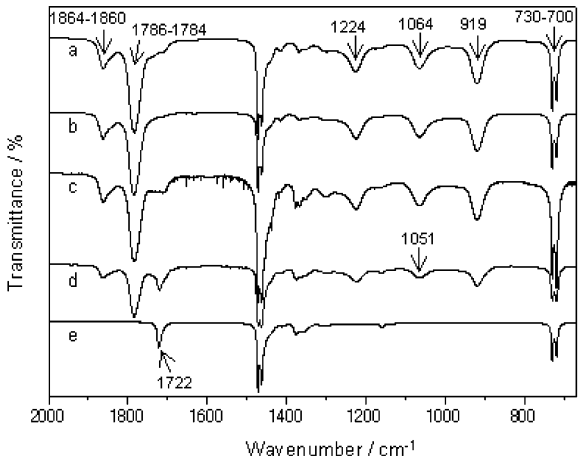

Figure 1. IR spectra of lmPE and MA-*g*-PE synthesized with an added MA amount of 20 wt % for PE for 1 h: MA-*g*-HDPE1 at 180 °C (a), MA-*g*-HDPE2 at 180 °C (b), MA-*g*-LDPE at 180 °C (c), [2,3-$^{13}C_2$] MA-*g*-lmPE at 170 °C (d), and lmPE (e).

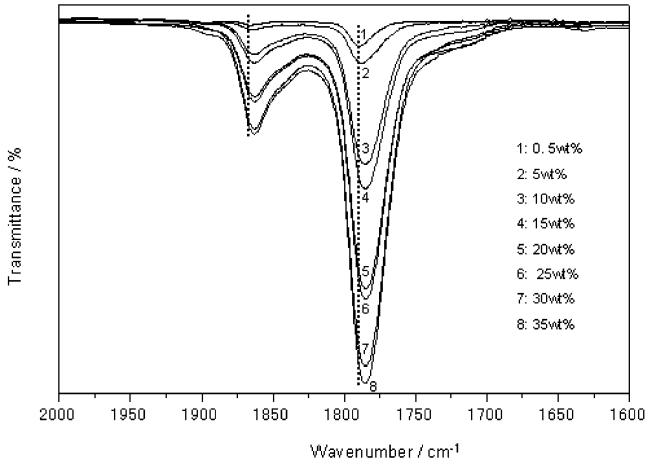

Figure 2. IR spectra of MA-*g*-HDPE2 synthesized with different MA amounts and DTBP/HDPE2 = 2 wt % at 180 °C for 1 h.

of aliphatic esters at 1722 cm^{-1} is assigned to the terminal initiator groups (−O−C(=O)−R) of the lmPE backbone (curves d and e).

We determined first the optimal conditions for synthesis of MA-*g*-PE from four kinds of PE (HDPE1, HDPE2, LDPE, and lmPE), focusing on the DTBP amount from 0.1 to 10 wt % of PE, the reaction temperature of 140−190 °C, and the reaction time of 0.5−2 h. The content of MA grafts was evaluated qualitatively from the area ratio of the IR band due to ν_s(C=O) (1790−1784 cm^{-1}) to that due to the CH_2 rocking of PE (730−700 cm^{-1}), as shown in Figure 1. Under the resultant optimal conditions, we synthesized MA-*g*-PE with a wide range of grafted MA content by changing the amount of added MA in order to examine in detail the variation of the structure of grafts with the content of grafted MA. Figure 2 shows IR spectra of MA-*g*-HDPE2, which samples were synthesized using amounts of added MA of 0−35 wt % with DTBP/HDPE2 = 2 wt % at 180 °C for 1 h. It is very interesting that ν_s(C=O) as well as ν_{as}(C=O) shifts to lower wavenumbers with an increase in the added MA amount. Similar results were observed for the other three kinds of MA-*g*-PE, suggesting a change in structure of grafts in MA-*g*-PE.

To determine the microstructure of grafted MA, high-resolution solution-state NMR spectroscopy has been successfully applied to [2,3-$^{13}C_2$]MA grafted lmPE, since its solubility is high enough to get NMR spectra at a lower temperature, e.g., 85 °C.

Structure of lmPE. A ^{13}C NMR spectrum of lmPE is shown in Figure 3a, with the assignments according to previous studies.[18,24−26] The spectrum indicates that lmPE possesses many branches, such as ethyl, propyl, butyl, amyl, and longer branches. Methine carbons (tertiary carbons) are certainly observed at 2.35 ppm in a ^1H NMR spectrum (Figure 3b).[27] Thus, the ratio of the methine carbons to the total carbons in lmPE is expected to be 1.7 mol % from the integration strengths. The presence of aliphatic ester groups from an initiator in the backbone is also confirmed by the NMR analysis, in agreement with the IR result. The resonances for methylene carbons α and β connected with −COOR is observed at 43.1 and 24.0 ppm, respectively (Figure 3a).[24] Moreover, the resonance for such methylene protons is observed at 2.10 ppm in Figure 3b.[27] No resonance of protons on double bond carbons is observed, showing very little double bond on the backbone of lmPE.

Structure of [2,3-$^{13}C_2$]MA-*g*-lmPE. (a) Oligo-SA. [2,3-$^{13}C_2$]MA-*g*-lmPE exhibits some characteristics in ^1H NMR and inverse-gated ^1H decoupled ^{13}C NMR spectra, quite different from those of lmPE. A COSY spectrum of [2,3-$^{13}C_2$]MA-*g*-lmPE is shown in Figure 4. In the 1 D ^1H NMR spectrum, three weak and broad peaks are observed at 3.24, 2.94, and 2.70 ppm. The former one is assigned to methine protons, and the latter two are due to methylene protons, in the terminal rings of structure **II** (oligo-SA) in Scheme 1, on the basis of the assignments on *n*-eicosane[28] and hept-4′-yl succinic anhydride.[29] The COSY spectrum shows a stronger correlation (plot 1) due to a geminal coupling of the methylene protons as well as a weaker correlation (plot 2) from a vicinal coupling of the methine proton and one of the methylene protons, both of which are in the same side with respect to the plane of the terminal ring. No signals due to the intermediate methine protons were observed in the ^1H NMR spectrum, although ^{13}C NMR spectra suggest strongly the formation of oligomeric grafts, as described soon later. The intermediate methine protons are less observable than the terminal protons because of more broadening of the peak due to the former protons.[30] A very weak and broad signal at 6.5 ppm is due to protons on double bond carbon,[31] as assigned below.

In the higher field of inverse-gated ^1H decoupled ^{13}C NMR spectra of [2,3-$^{13}C_2$]MA-*g*-lmPE in Figure 5, signals of oligo-SA appear at 32−30 and 46−42 ppm, which have been well assigned to the methylene carbon (C3 in structure **II**) on the terminal SA ring and methine carbons, respectively.[13,28,29,32,33] This assignment is consistent with an H, C-COSY 2D spectrum of [2,3-$^{13}C_2$]-MA-*g*-lmPE in Figure 6, where the axes F_1 and F_2 are for ^1H and ^{13}C chemical shifts, respectively. Plot 1 (F_2: 32−30 ppm) and plot 2 (F_2: 46−42 ppm) correlate well with methylene (F_1: 2.70 and 2.94 ppm) and methine protons (F_1: 3.24 ppm) in the ^1H NMR spectrum, respectively. Furthermore, it can be confirmed from a DEPT ^{13}C NMR spectrum (Figure 5) that the signal of the labeled ring methine at 46−42 ppm is up, while the signal of the labeled ring methylene at 32−30 ppm is down when θ is 135°.

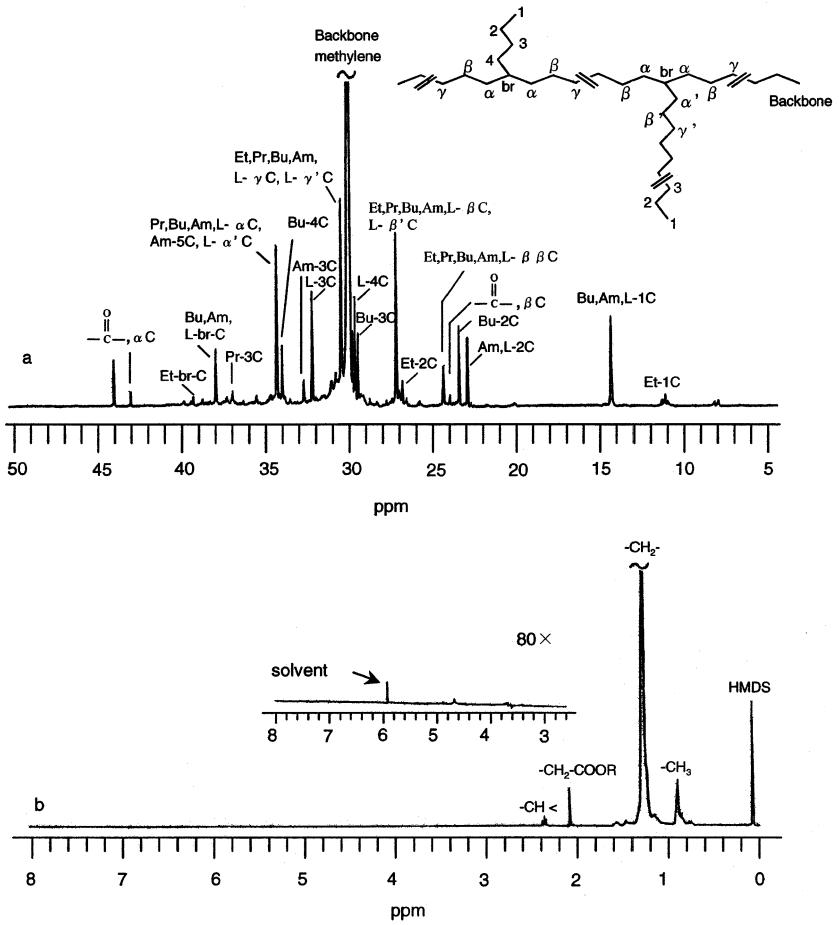

Figure 3. NMR spectra of lmPE at 85 °C in 1,1,2,2-tetrachloroethane-d_2: an inverse-gated ^{1}H decoupled ^{13}C NMR spectrum (a) and a ^{1}H NMR spectrum (b). Et = ethyl, Pr = propyl, Am = amyl, and L = longer chains (the length ≥ 6 carbons).

(b) Oligo-MA. For the lower field in Figure 5, we observed for the first time two new pairs of signals at about 158 and 128 ppm, which become broader with the added MA amount exceeding 10 wt % lmPE. They are characteristic of an AX spin system {$\Delta\nu/J$ = 46 (>6), where $\Delta\nu$ is the chemical shift difference between nuclei (2979.9 Hz) and J is the coupling constant (65.20 Hz)},[27] which indicates that there are inequivalent labeled carbons attached to lmPE chains. The value of J agrees with a directly bonded CC coupling ($^1J_{CC}$) for C=C double bonds.[31] It is noted that no such resonances are observed in a spectrum of unlabeled MA-*g*-lmPE (added ma/lmPE: 25 wt %). Therefore, the double bond is due to ^{13}C-labeled unsaturated graft anhydrides and not to the C=C double bonds that might generate on the branching lmPE backbone during the grafting process.[12] The number of such double bonds on the lmPE backbone is too small to be examined with ^{13}C NMR spectroscopy.

The H, C-COSY 2D analysis of [2,3-$^{13}C_2$]MA-*g*-lmPE is very effective for the assignment of the peaks at 158 and 128 ppm, as shown in Figure 6. Plot 3 with F_2 = 128 ppm has a correlated peak at F_1 = 6.5 ppm, which has already been assigned to a proton bound to a double bond carbon atom. However, the lack of a correlated ^{1}H peak with the ^{13}C signal at 158 ppm means the other double bond carbon is quaternary. Therefore, the NMR results show clearly that [2,3-$^{13}C_2$]MA-*g*-lmPE have graft groups with a terminal unsaturated maleic anhydride, i.e., oligo-MA, the same as structure **I** in Scheme 1.

It is very interesting in the lower field of Figure 5 that, although only a couple of sharp doublet signals at 158 and 128 ppm appear in the added MA amount up to 2 wt %, they are accompanied by two broad bands centered at the different chemical shifts, slightly smaller than 158 and a little greater than 128 ppm, in the added MA amount greater than 2 wt %. The more governing intensity of the broad bands than the sharp ones with increasingthe added MA content implies that the sharp signals may be due to the single grafts (m = 0), while the broad signals may be from the oligomeric grafts (m ≥ 1). The slight difference in chemical shift between the sharp and broad signals is indicative for such an assignment.

The chemical shifts, δ_{C2} and δ_{C3}, for the C2 and C3 atoms in the terminal ring of oligo-MA are estimated on the basis of the method for alkenes,[34] considering substitutions of −COOR but not a cyclic effect for oligo-MA.

$$\delta_{C2} = 123.3 + 10.6n_\alpha + 7.2n_\beta - 1.5n_\gamma + 6.0n_{\alpha(-COOR)} + 7.0n_{\alpha'(-COOR)} + S_{cis(\alpha\alpha')} + S_{\alpha\alpha} + S_{\beta\beta} \quad \text{(for } m = 0 \text{ and } m \geq 1\text{)}$$

and

$$\delta_{C3} = 123.3 + 6.0n_{\alpha(-COOR)} - 7.9n_{\alpha'} - 1.8n_{\beta'} + 1.5n_{\gamma'} + 7.0n_{\alpha'(-COOR)} + S_{cis(\alpha\alpha')} + S_{\alpha'\alpha'} \quad \text{(for } m = 0 \text{ and } m \geq 1\text{)}$$

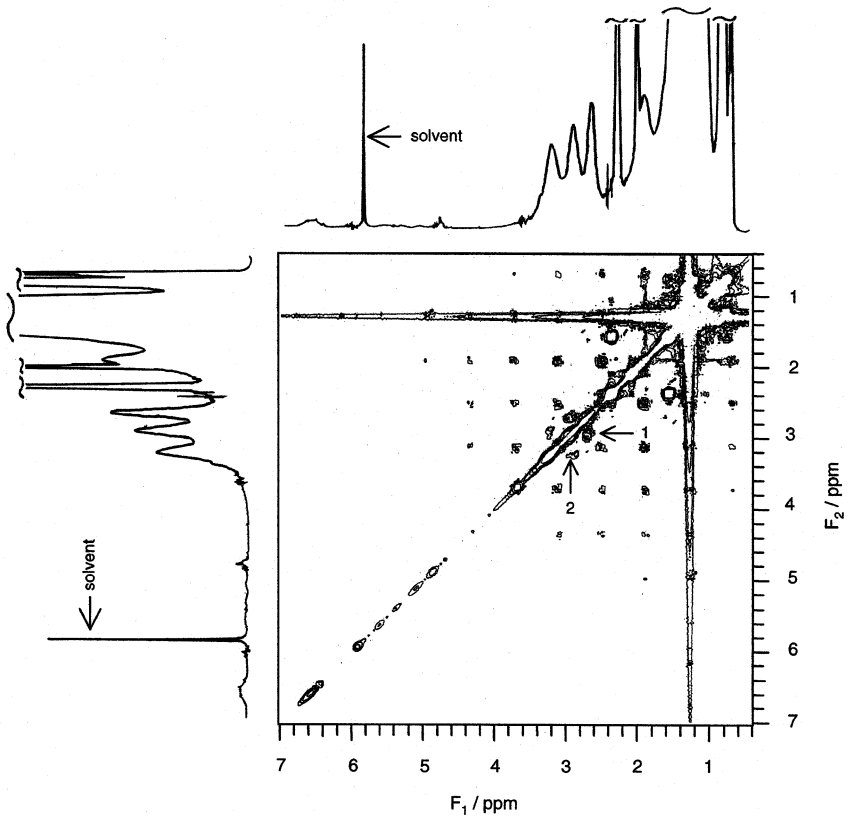

Figure 4. COSY spectrum of [2,3-$^{13}C_2$]MA-*g*-lmPE with an added MA amount of 25% for lmPE.

Table 1. Calculatd and Experimental Values of the Chemical Shifts for C2 and C3 on the Terminal Ring of Oligo-MA

	chemical shift (ppm)			
	C2		C3	
	$m = 0$	$m \geq 1$	$m = 0$	$m \geq 1$
calculated	154.7	149.0	129.2	129.5
observed[a]	158.0	156.8	128.4	129.3

[a] The values for the sharp and broad signals of C2 and C3 are listed in the columns with $m = 0$ and $m \geq 1$, respectively.

where α, β, and γ refer to the positions of carbons on the same side of the double bond as C2 or C3 under consideration and α', β', and γ' to those on the opposite side, and n_α ($n_{\alpha'}$), n_β ($n_{\beta'}$),and n_γ ($n_{\gamma'}$) are the numbers of the corresponding carbons. The value of 123.3 is the δ value for ethylene, and the correction terms have usual meanings: $S_{\mathrm{cis}(\alpha\alpha')} = -1.1$, $S_{\alpha\alpha} = -4.8$, $S_{\alpha'\alpha'} = 2.5$, and $S_{\beta\beta} = 2.3$.

The calculated results are summarized with the experimental ones in Table 1. The calculated δ_{C2} and δ_{C3} values for the oligomeric grafts ($m \geq 1$) are constant, not depending on the value of m. Further, the calculated δ_{C2} value for the oligomeric grafts is smaller than that for the single graft ($m = 0$), while the calculated δ_{C3} value for the oligomeric grafts is slightly greater than that for the single graft. The correspondence of these calculated results with the experimental ones (Table 1) suggests strongly that the sharp signals are assigned to the single grafts ($m = 0$) and the broad signals are due to the oligomeric grafts ($m \geq 1$).

(c) Why Are the Signals of the Graft Groups Broad? The above assignment of the signals at around 158 and 128 ppm indicates that oligomerization of the grafts oligo-MA and oligo-SA may cause the broadening of corresponding NMR signals. We can observe certainly that the signals at 45 and 32 ppm also become more broadening, particularly in the amount of added MA equal to and greater than 10 wt %. This expectation is supported by that, although hept-4′-yl succinic anhydride, a model for the single graft of oligo-SA, has very sharp ^{13}C NMR signals at 43.2 and 29.8 ppm,[29] synthesized poly(maleic anhydride) exhibited a very broad signal due to methine carbons at around 45 ppm.

Different from the single graft ($m = 0$ and $n = 0$), the diversity in configuration of the graft chains is more significant with increasing the degree of oligomerization ($m \geq 1$ or $n \geq 1$). The cis-type linkage of succinic anhydride units brings both meso-diisotactic and meso-disyndiotactic configurations for each unit with $m \geq 2$ ($n \geq 2$) on oligo-MA (oligo-SA), but only one meso-configulation for the unit with $m = 1$ on oligo-MA because of the planar terminal ring and two meso-type configurations for the unit with $n = 1$ on oligo-SA. Similarly, the trans-type linkage generates racemo-type configurations on oligo-MA and oligo-SA. The real configuration of oligo-MA and oligo-SA is more complexed than these extreme cases because each succinic anhydride unit can take the cis- or trans-type linkage. Further, the motion of such grafts is considerably restricted by the bulkiness of the monomeric ring units as well as by strong interactions between the polar rings and accordingly makes the molecular correlation time τ_c longer. Since the longer τ_c results in the shorter T_2, the spin−spin relaxation time, the signals due to the oligomeric grafts are expected to become broader because the half-height line width $\nu_{1/2}$ is expressed by the equation $\nu_{1/2} = 1/(\pi T_2)$.[31] Therefore, the broadening of the ^{13}C NMR signals in Figure 5 probably results from the diversity in configuration and the slow motion in

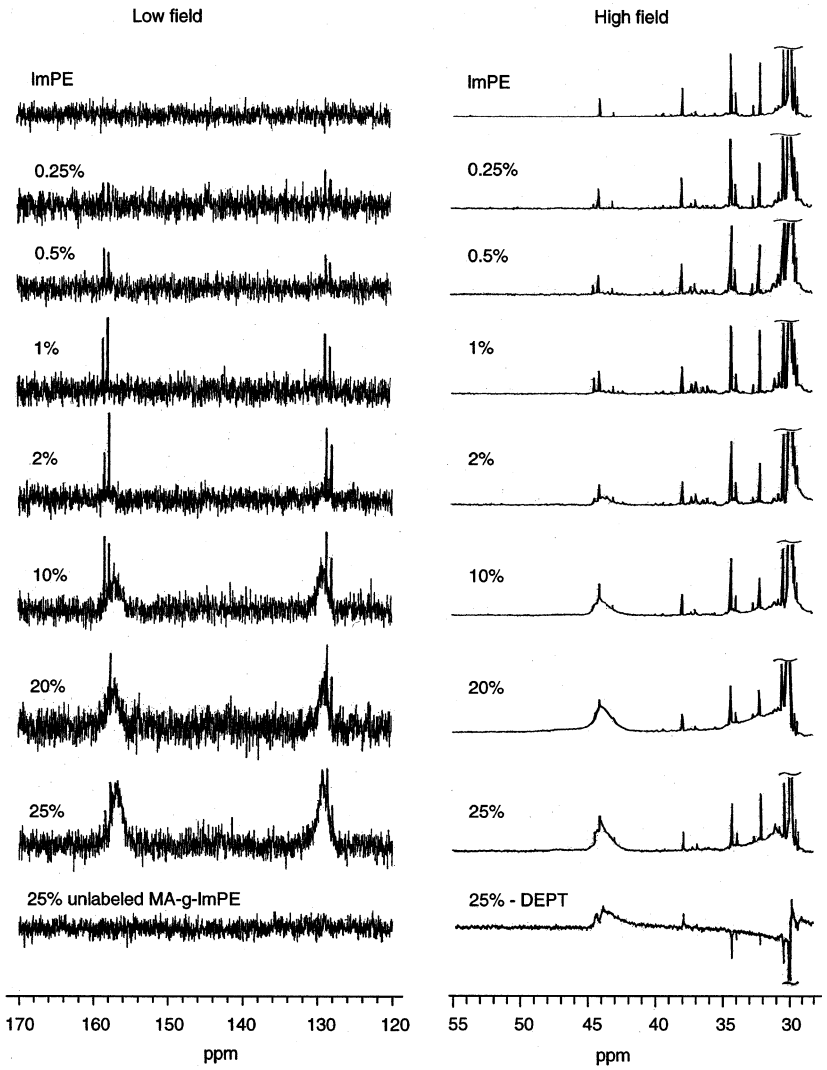

Figure 5. Inverse-gated ^{1}H decoupled ^{13}C NMR spectra of lmPE and [2,3-$^{13}C_2$]MA-*g*-lmPE with an added MA amount of 0.25−25 wt % for lmPE in the low and high fields at 85 °C in 1,1,2,2-tetrachloroethane-d_2, together with a DEPT spectrum with added MA/lmPE = 25 wt % as well as a reference of unlabeled MA-*g*-lmPE (added MA/lmPE: 25 wt %).

conformation change of the oligomeric grafts oligo-MA and oligo-SA.

The present results demonstrate clearly that [2,3-$^{13}C_2$]-MA-*g*-lmPE has oligo-MA with a terminal unsaturated ring (structure **I** in Scheme 1) as well as oligo-SA with a terminal saturated ring (structure **II** in Scheme 1), the only graft structure that had been observed prior to this work.[13] It is noted that oligo-MA is primarily the single type ($m = 0$) in the amount of added MA smaller than 2 wt %, beyond which it consists of the oligomeric types ($m \geq 1$) as well as the single one.

Quantitative Analysis of Oligo-MA and Oligo-SA. From the integrated responses in the inverse-gated ^{1}H decoupled ^{13}C NMR spectra (Figure 5) after correction for the lmPE background, we may estimate the graft average chain lengths of oligo-MA ($m + 1$) and oligo-SA ($n + 1$) and the molar ratio of oligo-MA to oligo-SA (R_M/R_S). For this examination, we make two assumptions: (1) the types of graft groups are oligo-MA and oligo-SA, and (2) the numbers of methine, methylene, and quaternary carbons in oligo-MA and oligo-SA are proportional to the integration strengths of the corresponding ^{13}C NMR peaks.

The structural features of oligo-MA and oligo-SA satisfy the following relations:

$$N_{CH} = N_{CH(M)} + N_{CH(S)} \quad (1)$$

$$N_{CH(M)}/N_{C3(M)} = N_{CH(M)}/N_{C2(M)} = 2m/1 \quad (2)$$

$$N_{CH(S)}/N_{C3(S)} = (2n + 1)/1 \quad (3)$$

where N is the number of carbons. The subscripts CH-(M) and CH(S) denote methine carbons in oligo-MA and oligo-SA, respectively, and the subscript CH is the total methine carbons in the grafts; the subscripts C2(M) and c3(M) denote the C2 and C3 carbons in oligo-MA, and the subscript C3(S) the C3 carbon in oligo-SA. From eqs 1−3, eq 4 is derived:

$$n + (N_{C3(M)}/N_{C3(S)})m = {}^1/_2(N_{CH}/N_{C3(S)} - 1) \quad (4)$$

On the basis of assumption (2), eq 4 is equivalent to the following relation:

$$n + (I_{C3(M)}/I_{C3(S)})m = {}^1/_2(I_{CH}/I_{C3(S)} - 1) \quad (5)$$

where I is the integrated carbon response. This equation shows the relation between the average chain lengths of oligo-MA and oligo-SA. In the added MA amount equal to and smaller than 2 wt %, the exact value of n

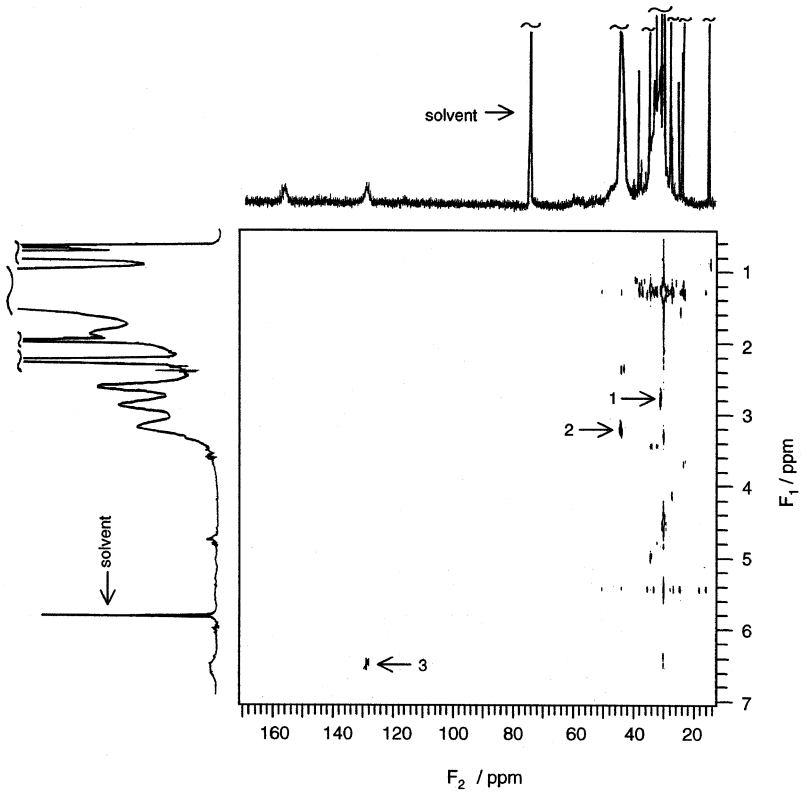

Figure 6. H,C-COSY spectrum of [2,3-$^{13}C_2$]MA-*g*-lmPE with an added MA amount of 25 wt % for lmPE.

Table 2. IR and Quantitative ^{13}C NMR Analyses of [2,3-$^{13}C_2$] MA-*g*-lmPE

run no.	added MA/lmPE (wt %)	added MA/DTBP (molar ratio)	$\nu_{s(C=O)}$ (cm^{-1})	$\nu_{as(C=O)}$ (cm^{-1})	GD2[a] (wt %)	*m*	*n*	R_M/R_S (molar ratio)
1[b]	0.25	0.037	1788.8	1863.6	0.012	0	0	
2[b]	0.5	0.074	1787.6	1861.9	0.063	0	0.19	
3	1	0.15	1787.0	1861.4	0.16	0	0.68	1/20
4	2	0.30	1786.8	1861.5	0.35	0	1.1	1/16
5	10	1.5	1785.6	1860.7	2.1	0−22	2.1−0	1/11
6	20	3.0	1784.6	1860.8	2.4	0−21	2.9−0	1/7.1
7	25	3.7	1784.0	1860.5	2.3	0−21	3.3−0	1/6.4

[a] GD2: The grafting degree is defined as the weight ratio of grafted MA to lmPE.[35] [b] The resonance of oligo-MA is too weak to integrate and further to calculate some parameters.

is obtained through eq 5 because oligo-MA is the single graft, i.e., $m = 0$, as discussed before; however, beyond the MA region, we cannot estimate the values of *m* and *n* exactly because oligo-MA as well as oligo-SA becomes oligomeric, and the signals due to the methine carbons of both grafts overlap each other at 46−42 ppm in the ^{13}C NMR spectra (Figure 5). On the other hand, the molar ratio of oligo-MA to oligo-SA, R_M/R_S, is given by eq 6:

$$R_M/R_S = N_{C3(M)}/N_{C3(S)} = I_{C3(M)}/I_{C3(S)} \qquad (6)$$

The average chain lengths of oligo-MA ($m + 1$) and oligo-SA ($n + 1$) and the molar ratio of oligo-MA to oligo-SA (R_M/R_S) are listed in Table 2. The value of *n* increases from 0 gradually with an increase in the add MA amount up to 2 wt %, in quite contrast to $m = 0$. For the amount of added MA greater than 2 wt %, *m* is greater than 0 because of the formation of oligomeric grafts for oligo-MA, as shown in Figure 5. The most remarkable observation is that oligo-MA grafts are fewer than oligo-SA grafts in MA-*g*-lmPE, although the molar ratio R_M/R_S increases with an increase in the added MA amount. It is noted from the quantitative analysis that the number of grafted MA monomers,

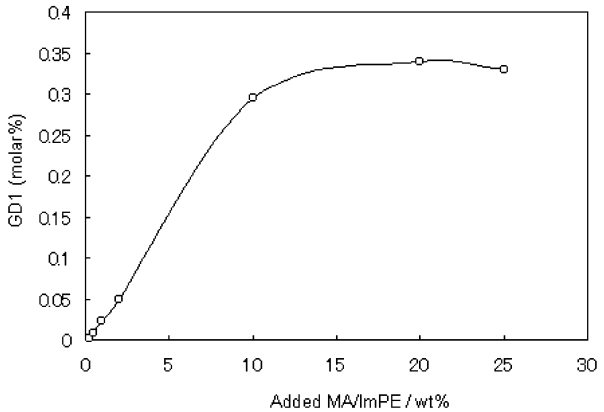

Figure 7. Relation between the grafting degree (GD1) and the added MA amount.[35]

GD1, goes up to 3−4 per 1000 carbons on the PE backbone (Figure 7), and accordingly the grafting degree, GD2, increases to about 2.3 wt % lmPE, as shown in Table 2.[35] The grafting degree is smaller than the value obtained in the case with HDPE.[13]

Lower Shift of the Symmetric and Asymmetric Stretching Vibration of C═O with the Increase of

Scheme 2. Resonance Structure of Grafted Anhydride Moiety and the Probable Interaction Mode

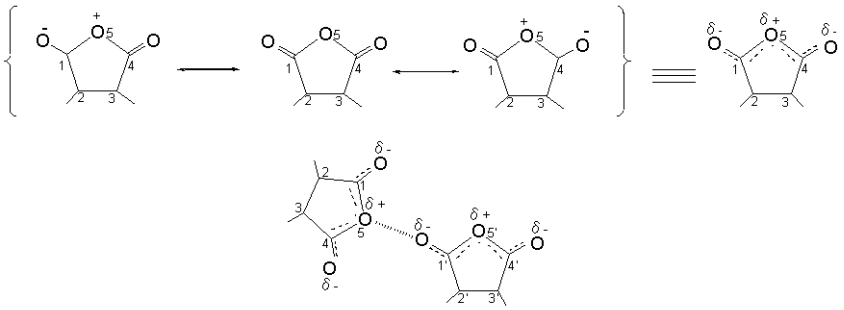

Grafted Anhydride Groups. Two compounds were chosen as model compounds for grafted anhydride of MA-*g*-PE in IR analysis: one is *n*-octadecylsuccinic anhydride which contains a single anhydride graft with ν_s(C═O) of 1792 cm^{-1} and ν_{as}(C═O) of 1867 cm^{-1}; the other is synthesized poly(MA) with ν_s(C═O) of 1780 cm^{-1} and ν_{as}(C═O) of 1851 cm^{-1}. These examples suggest that the carbonyl stretching of a single anhydride graft is at a higher wavenumber than that of a multiple anhydride graft. With an increase in the added MA amount, the grafting degree GD2 increases, and the carbonyl stretching vibrations shift to the lower wavenumbers (Table 2), probably due to the increase in the average grafting chain length or the number of grafting sites.

Resonance theory indicates that a grafted anhydride moiety can be polarized to yield a positive charge on O5 and a negative charge on O1 and O4 in Scheme 2. This polarization of anhydride may induce the interaction between the O5 atom of a grafted anhydride moiety and the O1′ or O4′ atom of another grafted anhydride moiety, particularly in a solid state. Such interaction may be more probable between different longer graft chains than in a chain, considering the conformation or configuration of the graft chains. From Scheme 2, the stronger interaction polarizes a pair of interacting grafted anhydride moieties to decrease the bond order of C═O. Accordingly the stronger interaction may cause the symmetric and asymmetric C═O stretching vibrations to make a lower shift with an increase in the content of grafted anhydride groups.

A Mechanism for the Formation of Oligo-MA. We have demonstrated from ^{13}C NMR spectroscopy that MA-*g*-lmPE contains SA oligomeric grafts with a terminal MA ring (oligo-MA) in addition to SA oligomeric grafts terminating in a saturated SA ring (oligo-SA) and that oligo-MA groups are fewer than oligo-SA groups, as shown in Table 2. It is worth noting that the oligo-MA grafts are primarily the single type ($m = 0$) in the smaller amount of added MA and contain much more oligomeric types ($m \geq 1$) with the greater MA amount, while the oligo-SA grafts tend to be oligomeric types. Our interest is focused on the clarification of the mechanism through which oligo-MA, the new graft groups, is formed in the grafting of MA onto lmPE.

Before considering the grafting mechanism of MA onto lmPE, we note that the hydrogen atom on a tertiary carbon is abstracted more readily than one on a secondary carbon; conversely, a radical on a secondary carbon causes the hydrogen abstraction more easily than does that on a tertiary carbon.[12] The present backbone polymer, lmPE, is expected to contain branching sites (tertiary carbons) equal to about 1.7 mol % of the total carbons on lmPE, as described above. However, in the grafting of MA onto lmPE, we may consider that the macroradicals are formed almost entirely on secondary carbons on lmPE and that the termination of grafting is largely governed by the hydrogen abstraction from secondary carbons because, according to Heinen et al.,[13] even the grafting of MA onto LDPE with a ratio of ethene to propene units of 12/1 (the fraction of the tertiary carbons to the total carbons on the LDPE main chain is 3.85 mol %) is almost the same as that onto HDPE, both yielding only oligo-SA on secondary carbons. Accordingly, we examined the beginning steps for grafting of MA onto lmPE on the basis of the mechanism with HDPE.[13] First, macroradicals are formed on secondary carbons of lmPE to cause the grafting of MA monomers there. MA being a strong electron acceptor causes a great number of the monomeric grafting radicals to abstract hydrogen atoms from methylene carbons on lmPE to yield single MA grafts, on account of the intra- and intermolecular hydrogen transfers. But because of the slight effect of tertiary carbons with lmPE, quite different from the cases of alternative ethene−propene copolymer and PP that yield only the single grafts,[13] the surviving monomeric grafting radicals further graft MA monomers to produce (k+1)-fold oligomeric radicals, oligo-R(k+1). The radicals oligo-R(k+1) are also terminated similarly by the hydrogen abstraction from lmPE to yield oligo-SA with a degree of grafting = $k + 1$, oligo-SA(k+1). However, the above mechanism, which is the same as the grafting mechanism presented by Heinen et al.,[13] cannot explain the formation of oligo-MA.

Another termination process is required to understand the formation of oligo-MA. The longer the radicals oligo-R(k+1) are, the more readily they may interact with each other, as discussed earlier. Such interaction is favorable for disproportionation between oligo-R(k+1) and another radical oligo-R(l+1) and unfavorable for the hydrogen abstraction of oligo-R(k+1) from lmPE. It is noted that this disproportionation yields naturally oligo-MA(k+1) and oligo-SA(k+1) with the same probability. Another disproportionation can occur between oligo-R(k+1) and a radical site on lmPE (Scheme 3). Scheme 3 shows that there are two different modes of disproportionation: one is the attack of a radical (1′) on lmPE at H (2) of oligo-R(k+1) to yield oligo-MA(k+1) and alkane (mode I), and the other is, conversely, the attack of the radical site (3) on oligo-R(k+1) at H (2′) of lmPE to produce oligo-SA and alkene (mode II). We note in Scheme 3 that H (2) is located on a tertiary carbon, while H (2′) is placed on a secondary carbon, with the positioning of the radical sites (3 and 1′) on a secondary carbon. Because of the easier abstraction of a hydrogen atom on a tertiary carbon than on a secondary one, we can reasonably expect that mode I of disproportionation

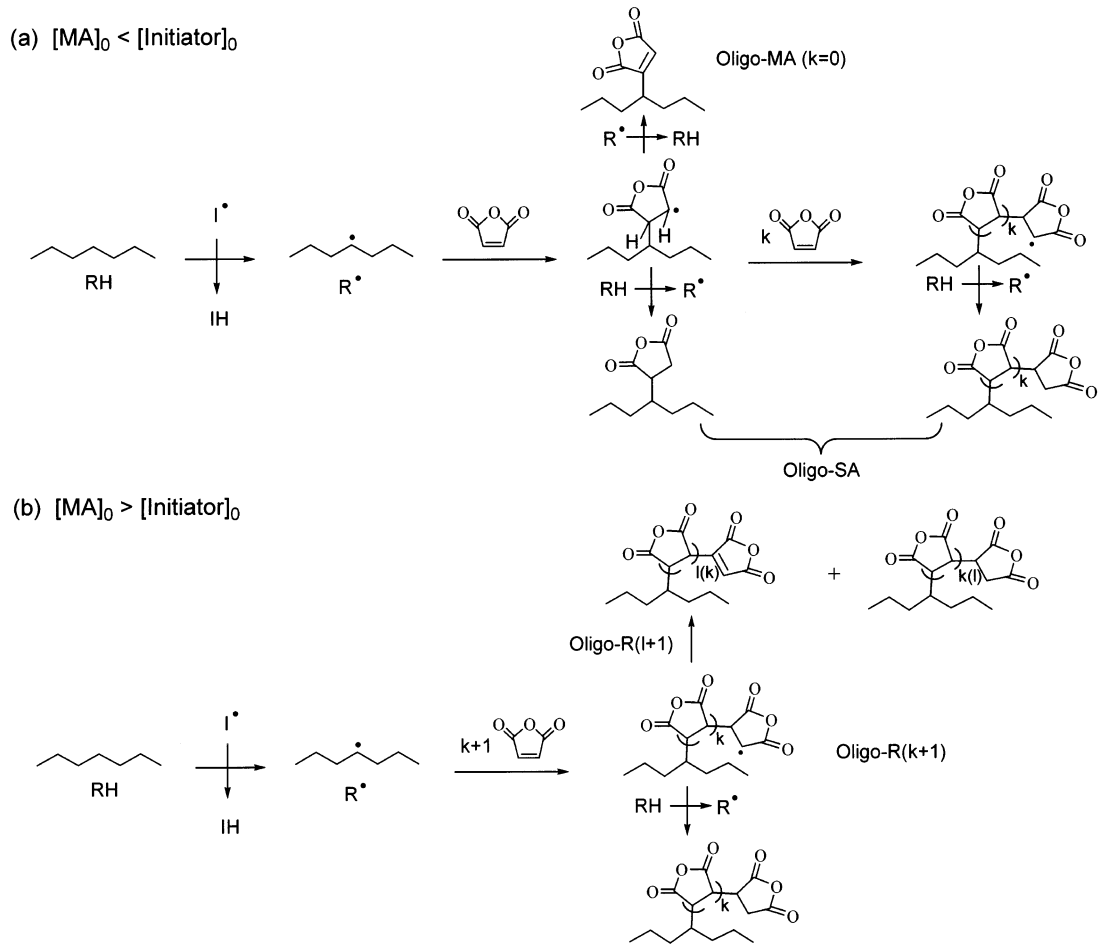

Figure 8. Grafting mechanism of MA onto lmPE to yield oligo-MA as well as oligo-SA. I• denotes an initiator, R a lmPE chain, and R• a macroradical.

Scheme 3. Disproportionation between Oligo-R(*k*+1) and a Radical Site on a Secondary Carbon in LmPE To Cause the Predominant Formation of Oligo-MA (Mode I) or Oligo-SA (Mode II)

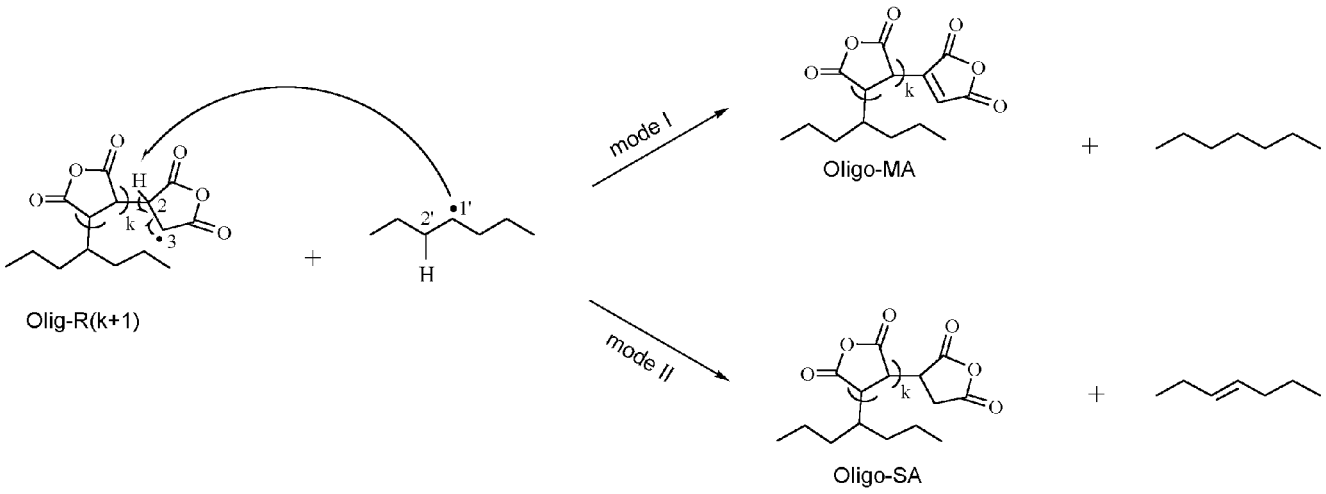

is more probable than mode II. We recall that mode I is the disproportionation to terminate oligo-R(*k*+1) into oligo-MA(*k*+1).

A brief mechanism for the grafting of MA onto lmPE is shown in Figure 8. For the molar quantity of added MA smaller than that of the initiator (corresponding to runs 1−4 in Table 2; Figure 8a), the formation of the single radicals oligo-R(0+1) is considered as a key step, with excess formation of macroradicals on lmPE. Because of the relatively smaller quantity of added MA, the further grafting of MA monomers on the single radicals is restricted strongly to yield shorter oligo-SA by abstraction of a hydrogen atom on lmPE. Disproportionation between the surviving single radicals and macroradicals on lmPE is also probable to yield the single graft for oligo-MA because of the excess formation of such macroradicals in the beginning step as well as because of expected stabilization of the single radical due to the formation of a six-membered ring transition state (Scheme 4). Even disproportionation between the

Scheme 4. Expected Formation of a Six-Membered Ring Transition State by the Single Radical

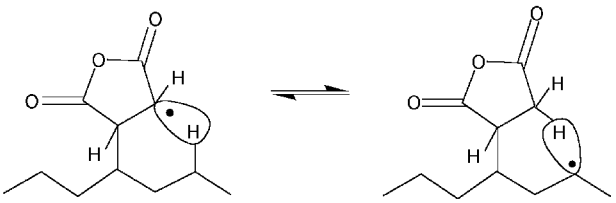

single radical and the longer radical oligo-R(k+1) would generate oligo-MA(0+1) and oligo-SA(k+1) more than the opposite species because the transition state of the single radical probably reduce the power for hydrogen abstraction of the radical site on C3, different from the longer radicals which are difficult to form such a transition state.

With an increase in the molar quantity of added MA (related to runs 5−7 in Table 2; Figure 8b), the formation of longer graft radicals oligo-R(k+1) is more probable. Accordingly, the longer radicals may yield the longer oligo-SA by hydrogen abstraction from lmPE. Since the longer radicals may interact with each other more readily, the possibility of disproportionation between the radicals increases to generate oligo-MA(k+1) and oligo-SA(k+1) with the same probability. Thus, the molar ratio of oligo-MA to oligo-SA increases with increasing the chain length of the grafts.

Therefore, the mechanism with two different termination processes explains concisely the result that MA-*g*-lmPE contains fewer oligo-MA with a terminal unsaturated MA ring as well as more oligo-SA terminating in a saturated SA ring, with an increasing molar ratio of oligo-MA to oligo-SA. This mechanism is effective for explaining that only the single graft for oligo-MA is generated with oligomeric grafts for oligo-SA in the smaller quantity of added MA than that of the initiator.

Conclusion

[2,3-$^{13}C_2$]MA-*g*-lmPE has fewer oligo-MA grafts with a terminal unsaturated MA ring as well as more oligo-SA grafts consisting of only saturated succinic anhydride rings. The formation of not only oligo-MA but also oligo-SA grafts can be explained on the basis of two different termination processes: disproportionation between a grafting radical and a macroradical on a secondary carbon in lmPE or another grafting radical as well as the hydrogen abstraction of a grafting radical from a secondary carbon in lmPE. The lower shift of the carbonyl symmetric and asymmetric stretchings in MA-*g*-PE with an increase in the grafting degree suggests stronger interactions between the grafts.

Acknowledgment. T. H. greatly appreciates Dr. H. Morii (Institute for Biological Resources and Functions, National Institute of Advanced Industrial Science and Technology) for his helpful discussions on the structural analysis of the grafts.

References and Notes

(1) Zhang, F. R.; Qiu, W. L.; Yang, L. Q.; Endo, T.; Hirotsu, T. *J. Mater. Chem.* **2002**, *12*, 24.
(2) Zhang, F. R.; Endo, T.; Kitagawa, R.; Kabeya, H.; Hirotsu, T. *J. Mater. Chem.* **2000**, *10*, 2666.
(3) Zhang, F. R.; Kabeya, H.; Kitagawa, R.; Hirotsu, T.; Yamashita, M.; Otsuki, T. *J. Appl. Polym. Sci.* **2000**, *77*, 2278.
(4) Zhang, F. R.; Kabeya, H.; Kitagawa, R.; Hirotsu, T.; Yamashita, M.; Otsuki, T. *Chem. Mater.* **1999**, *11*, 1952.
(5) Zhang, F. R.; Endo, T.; Qiu, W. L.; Yang, L. Q.; Hirotsu, T. *J. Appl. Polym. Sci.* **2002**, *84*, 1971.
(6) Yang, L. Q.; Zhang, F. R.; Endo, T.; Hirotsu, T. *Polymer* **2002**, *43*, 2591.
(7) Gaylord, N. G.; Mehta, R.; Mohan, D. R.; Kumar, V. *J. Appl. Polym. Sci.* **1992**, *44*, 1941.
(8) Liu, N. C.; Baker, W. E.; Russell, K. E. *J. Appl. Polym. Sci.* **1990**, *41*, 2285.
(9) Samay, G.; Nagy, T.; White, J. L. *J. Appl. Polym. Sci.* **1995**, *56*, 1423.
(10) Vito, G. D.; Lanzetta, N.; Maglio, G.; Malinconico, M.; Musto, P.; Palumbo, R. *J. Polym. Sci., Polym. Chem. Ed.* **1984**, *22*, 1335.
(11) Gaylord, N. G.; Mehta, M. *J. Polym. Sci., Polym. Lett. Ed.* **1982**, *20*, 481.
(12) Malaika, S. A. In *Reactive Modifiers for Polymers*, 1st ed.; Hu, G. H., Flat, J. J., Lambla, M., Eds.; Blackie Academic & Professional: London, 1997.
(13) Heinen, W.; Rosenmoller, C. H.; Wenzel, C. B.; de Groot, H. J. M.; Lugtenburg, J.; van Duin, M. *Macromolecules* **1996**, *29*, 1151.
(14) Gaylord, N. G.; Mehta, M.; Mehta, R. *J. Appl. Polym. Sci.* **1987**, *33*, 2549.
(15) Roover, B. D.; Sclavons, M.; Carlier, V.; Devaux, J.; Legras, R.; Momiaz, A. *J. Polym. Sci., Part A: Polym. Chem.* **1995**, *33*, 829.
(16) Sclavons, M.; Carlier, V.; Roover, B. D.; Franquinet, P.; Devaux, J.; Legras, R. *J. Appl. Polym. Sci.* **1996**, *62*, 1205.
(17) Regel, W.; Schneider, C**.** *Makromol. Chem.* **1981**, *182*, 237.
(18) Griselda, B. G.; Roberto, F. S.; Raquel, S. M.; Fernanda, F. N. *Macromolecules* **1999**, *32*, 1620.
(19) Canet, D.; Levy, G. C.; Peat, I. R. *J. Magn. Reson.* **1975**, *18*, 199.
(20) Wu, J. G. In *Techniques and Applications of Modern FTIR Spectroscopy*, 1st ed.; Xu, Z., Li, X., Wang, Z., Xi, S., Shen, X., Ruan, Z., Eds.; Science Press: Beijing, 1994; Vol. 1.
(21) Zhou, T. H. In *Handbook of Analysis Chemistry, No. 3: Spectroscopy Analysis*, 2nd ed.; He, Y. J., Dong, H. R., Eds.; Chemical Industry Press: Beijing, 1998.
(22) Gonzalez de los Santos, E.; Gonzalez, M. J. L.: Gonzalez, M. C. *J. Appl. Polym. Sci.* **1998**, *68*, 45.
(23) Silverstein, R. M. In *Spectrometric Identification of Organic Compounds*; Wiley: New York, 1981.
(24) Randall, J. C. *Macromol. Chem. Phys.* **1989**, *C29*, 201.
(25) Liu, W.; Ray, D. C., III; Rinaldi, P. L. *Macromolecules* **1999**, *32*, 3817.
(26) Wood-Adams, P. M.; Delay, J. M.; Willem deGroot, A.; David, R. O. *Macromolecules* **2000**, *33*, 7489.
(27) Ling, Y. C. In *Structural Identification of Organic Compounds and Organic Spectroscopy*, 2nd ed.; Science Press: Beijing, 2000.
(28) Russell, K. E.; Kelusky, E. C. *J. Polym. Sci., Part A: Polym. Chem.* **1988**, *26*, 2273.
(29) Heinen, W.; Erkens, S. W.; van Duin, M.; Lugtenburg, J. *J. Polym. Sci., Part A: Polym. Chem.* **1999**, *37*, 4368.
(30) Russel, K. E. *J. Polym. Sci., Part A: Polym. Chem.* **1995**, *33*, 555.
(31) Abraham, R. J.; Fisher, J.; Loftus, P. In *Introduction to NMR Spectroscopy*; John Wiley & Sons: New York, 1999.
(32) Ranganatgan, S.; Baker, W. E.: Russell, K. E.; Whitney, R. A. *J. Polym. Sci., Part A: Polym. Chem.* **1999**, *37*, 1609.
(33) Ranganatgan, S.; Baker, W. E.; Russell, K. E.; Whitney, R. A. *J. Polym. Sci., Part A: Polym. Chem.* **1999**, *37*, 3817.
(34) Wehrli, F. W.; Marchand, A. P.; Wehrli, S. In *Interpretation of Carbon-13 NMR Spectra*, 2nd ed.; John Wiley & Sons: New York, 1988.
(35) The molar ratio of grafted MA monomers to carbons on the main chain of lmPE, GD1, is defined as GD1 (mol %) = 1.108-[Σ*I* (the labeled carbons on the grafts)/2]/[Σ*I* (the carbons on the main chain of lmPE)], considering the ^{13}C content of the labeled [2,3-$^{13}C_2$] MA = 99%, the natural content of ^{13}C = 1.108%, and was calculated from the ^{13}C NMR signal intensity *I*. Thus, assuming that the average weight of carbon moieties on lmPE is equal to the weight of CH_2 (i.e., 14), the grafting degree, GD2, is expressed by GD2 (wt %) = 7GD1.

MA020527R